C. R. Mecanique 344 (2016) 797–806

Contents lists available at ScienceDirect

Comptes Rendus Mecanique

www.sciencedirect.com

Resin injection in clays with high plasticity

Hossein Nowamooz

ICUBE, UMR 7357, CNRS, INSA de Strasbourg, 24, boulevard de la Victoire, 67084 Strasbourg, France

ARTICLE INFO

Article history:
Received 21 January 2016
Accepted 5 September 2016
Available online 23 September 2016

Keywords:
Resin injection
Cavity expansion
Pressuremeter tests
Cone penetration tests

ABSTRACT

Regarding the injection process of polyurethane resins in clays with high plasticity, this paper presents the experimental results of the pressuremeter and cone penetration tests before and after injection. A very important increase in pressure limit or in soil resistance can be observed for all the studied depths close to the injection points. An analytical analysis for cylindrical pore cavity expansion in cohesive frictional soils obeying the Mohr–Coulomb criterion was then used to reproduce the pressuremeter tests before and after injection. The model parameters were calibrated by maintaining constant the elasticity parameters as well as the friction angel before and after injection. A significant increase in cohesion was observed because of soil densification after resin expansion. The estimated undrained cohesions, derived from the parameters of the Mohr–Coulomb criterion, were also compared with the cone penetration tests. Globally, the model predictions show the efficiency of resin injection in clay soils with high plasticity.

1. Introduction

Over the years, there has been considerable development in the stabilizing of cracking or jointed building structures. More and more engineers are being asked to address this often worrying problem. Some causes of this structural crack phenomenon are differential subsidence caused by the expansion or modification of building structures, and variations in the permanent weight distribution applied to that structure. In other circumstances, the cause of collapse can be ascribed to geotechnical property variations of the foundation soils: for instance, those caused by variations in the level of the water table in the area, by chemical degradation of some lithological compositions, or by leakage from buried pipes. Sometimes, mechanical improvement of foundation soils may also be required when changes in existing buildings have to be carried out by an elevation or variation in the supporting structure.

A recently proposed method is based on using polyurethane expanding resins, which are injected into the subsoil beneath the base of a shallow foundation [1–4]. In most cases, this type of remediation technique is performed without a preliminary design procedure and only on the basis of experience, i.e. this technique is merely an empirical approach.

Polyurethane resins belong to the category of foam materials, whose common attributes are high porosity, light weight, high crushability, and good deformation energy absorption capacity. These resins are essentially made of interconnected networks of solid struts and cell walls interspersed by voids with entrapped gas, and are generally classified as either open or closed cell foams [1,5]. It must be mentioned that there have been studies on the mechanical properties of polyurethane resins that have been extensively documented over the last two decades [6–8].

E-mail address: hossein.nowamooz@insa-strasbourg.fr.

http://dx.doi.org/10.1016/j.crme.2016.09.001

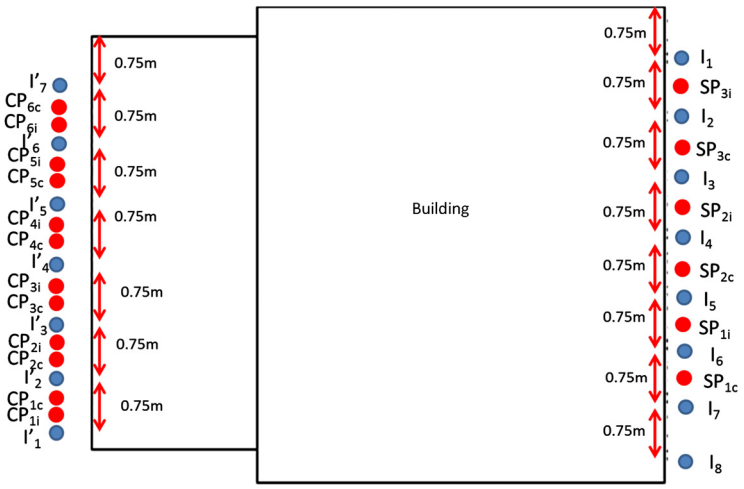

Fig. 1. Experimental platform in Noailles (Oise, France) before and after injection.

To study the field effect of resin injection in soils, in situ tests such as pressuremeter tests [9] or cone penetration tests [10] are necessary to be performed before and after injection. The reported test results in sandy soils showed the positive effect of the resin injection [11,12], but further investigations are still necessary for clays, particularly for clays with high plasticity.

Furthermore, the analysis of a cylindrical or spherical cavity has been applied to practical problems such as the interpretation of pressuremeter tests, the bearing capacity of deep foundations, and the installation of the driven piles [13–26].

In this context, this paper presents some in situ experimental results in a clay soil with high plasticity at different depths before and after injection. The pressuremeter results were modeled using an analytical analysis developed for cylindrical pore cavity expansion in Mohr–Coulomb cohesive frictional soils. The estimated undrained cohesions were also compared with cone penetration tests.

2. Experimental results

A series of experimental investigations on resin injection in plastic clays was performed in summer 2012 in Noailles, near Paris, France. The experimental platform is presented in Fig. 1. The identification tests showed the presence of more than 95% of clay till a depth of 4 m. The samples at the depth of 3 m show a liquidity limit (w_l) between 70.5% and 86%, and a plasticity limit (w_p) between 30% and 34%. The studied soils (till 4 m) were classified as clay with high plasticity (CH) based on the Unified Soil Classification System (USCS).

Three pressuremeter tests (symbolized by SP_i in Fig. 1) at the right-hand side of the building and six cone penetration tests (symbolized by CP_i in Fig. 1) at its left-hand side were performed before injection. The polyurethane resins were injected in eight points at the right-hand side of the building (symbolized by I in Fig. 1) and in seven points at its left-hand side (symbolized by I' in Fig. 1). The injections were performed at three different depths: 1.5 m, 2.5 m, and 3.5 m, where the radius of the injection tube was about 10 cm. Table 1 summarizes the injected masses of resin for each core at the different depths. The average injected masses of resin are 27.3 kg at the depth of 1.5 m, 43.5 kg at the depth of 2.5 m, and 19.3 kg at the depth of 3.5 m.

After injection, three pressuremeter tests (symbolized by SP_c in Fig. 2) and six cone penetration tests (symbolized by CP_c in Fig. 1) were performed to investigate the efficiency of resin injection in clays with high plasticity.

2.1. Pressuremeter tests

Fig. 2a shows the pressuremeter results (the variation of volume change with the applied pressure) before injection (cores SP_{1i}, SP_{2i} and SP_{3i}) at different depths: 1.5 m, 2.5 m, 3.3 m, and 4.2 m. These points were selected close to the future injection points 1.5 m, 2.5 m, and 3.5 m. The results show the increase in pressure limits at depth up to 2.5 m followed by a significant decrease in this value at the depth of 3.3 m before reaching its highest value at the depth of 4.2 m.

Fig. 2b also shows the pressuremeter results after injection (cores SP_{1c}, SP_{2c} and SP_{3c}) at the same positions. The same variation of pressure limits with depth obtained before injection can be observed after injection.

The results show globally an important increase in pressure limits for the studied depths compared with those obtained before injection.

Table 1
Mass of resin injected at three different depths in the studied cores.

Core	Injected mass (kg) at a depth of 1.5 m	Injected mass (kg) at a depth of 2.5 m	Injected mass (kg) at a depth of 3.5 m
I1	30	44	17
I2	31	43	15
13	40	49	14
I4	27	46	25
I5	24	61	20
I6	29	33	14
I7	34	38	15
I8	33	36	16
I'1	15	3	40
I'2	42	57	25
I'3	10	74	25
I'4	2	54	2
I'5	34	43	15
I'6	22	57	19
I'7	36	14	28
Average mass (kg)	27.3	43.5	19.3

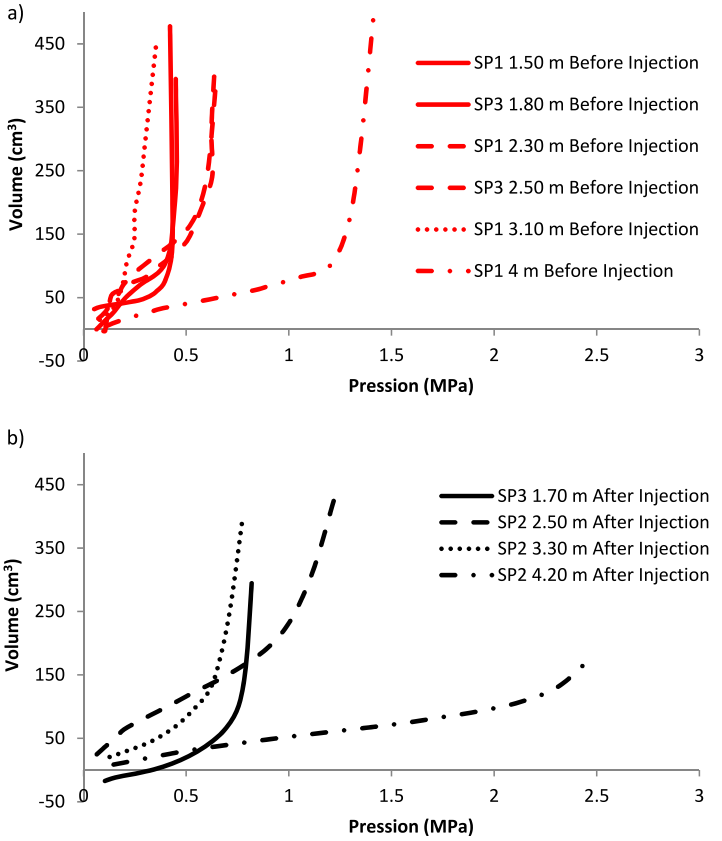

Fig. 2. Pressuremeter results a) before injection and b) after injection.

2.2. Cone penetration tests

Additionally, six cone penetration tests were performed before and after injection. Fig. 3 shows the experimental results (variation of soil resistance with depth) for CP_{1i}, CP_{1c}, CP_{4i} and CP_{4c} tests.

Fig. 3a shows that the soil resistance is the same in cores before injection, confirming the homogeneity of the studied clay in all cores. The remaining tests CP_{2i}, CP_{3i}, CP_{5i}, and CP_{6i} also evidence the same results.

After injection (Fig. 3b), resistance increases in both cores till the depth of 2.5 m. For the depths higher than 2 m, soil resistance reaches a very high value in CP_{1c} after injection, probably because of a resin slice as an obstacle on the penetration path and, therefore, the penetration was not possible to be continued. The same results were observed for the

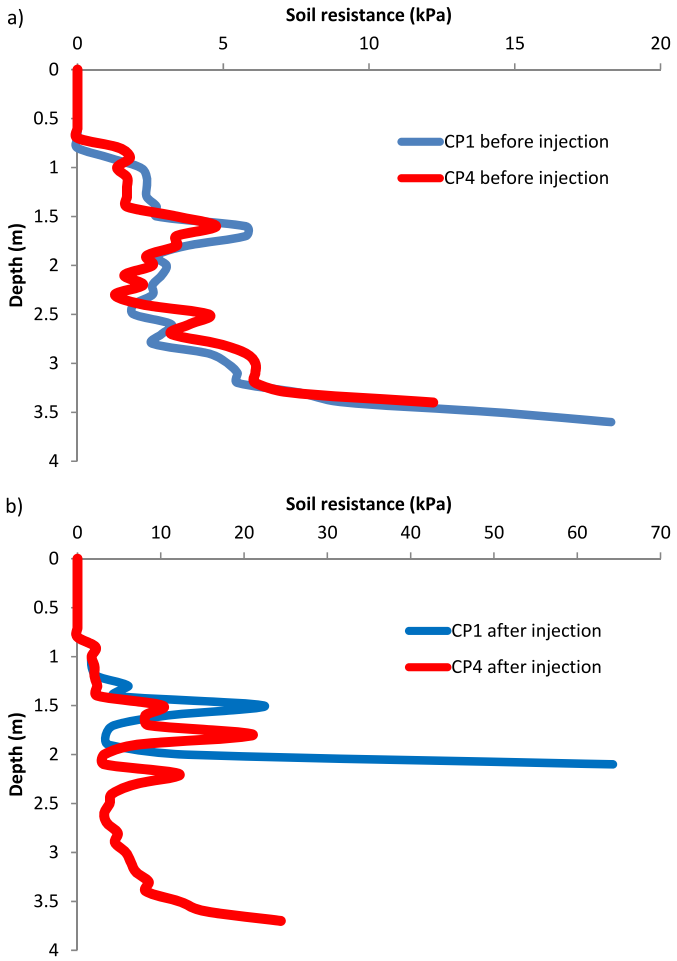

Fig. 3. Cone penetration results a) before injection and b) after injection.

CP_{2c}, CP_{3c}, CP_{5c}, and CP_{6c} tests. The only fulfilled cone penetration test till a depth of 4 m after injection was for CP_{4c}, for which the volumes of injected resin were less important than the average ones in the adjacent cores (see the injected masses in cores I'4 and I'5 in Table 1).

These results show the direct effect of the resin quantity on the mechanical behavior of the soils. In this work, the whole analysis will be based on the average injected volume, since the distance between the injection cores was taken constant (0.75 m). The injected volume may modify the necessary distance between the injection cores.

3. Analysis of the cavity expansion for the pressuremeter tests

The expansion process of the pressuremeter test in the soil can be theoretically studied as a cylindrical cavity expanding in quasi-static conditions. In this context, we follow the analytical solution developed by Carter et al. [20] for a cylindrical cavity expansion in a cohesive frictional soil obeying the Mohr–Coulomb criterion.

The behavior of the cylindrical cavity is described in terms of cylindrical polar co-ordinates (r, θ, z). It can be assumed that σ_r, σ_θ and σ_z are the principal stress components in cylindrical coordinates. The expansion of the cylindrical cavity occurs under conditions of plane strain and, provided that σ_z remains the intermediate principal stress and that there is no component of plastic strain in the z direction, the increase in σ_z can be calculated from

$$\Delta\sigma_z = \nu(\Delta\sigma_r + \Delta\sigma_\theta) \tag{1}$$

where ν is Poisson's ratio and all shear components of stress in the system are zero.

It will be assumed that the cavity is expanded in an infinite medium that is initially in a mean stress state $p_0 = (1 + 2k_0)\sigma_{z0}/3$, i.e. $\sigma_{r0} = \sigma_{\theta 0} = p_0$, where σ_{z0} is the initial vertical stress and k_0 is the coefficient of earth pressure at rest estimated by Jacky's equation:

$$k_0 = 1 - \sin\phi \tag{2}$$

where ϕ is the friction angle.

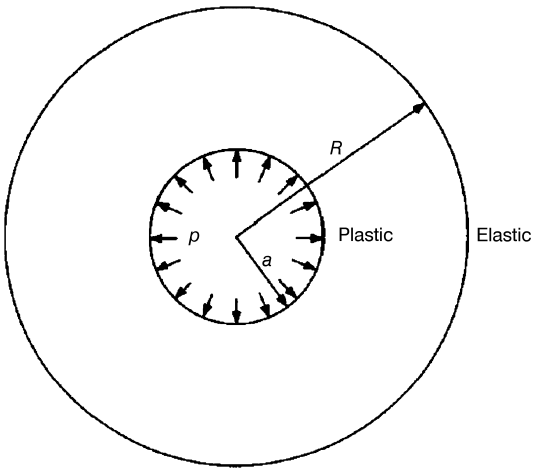

Fig. 4. Cavity expansion problem.

Hence conditions of axial symmetry and plain strain hold for the expansion of a cylindrical cavity, which greatly simplifies the analysis and allows a one-dimensional description of the problem because the displacements in the medium are everywhere radial. Since large deformations may occur, the radial co-ordinate of a typical particle may change significantly during the course of cavity expansion. The problem will involve both geometric and material nonlinearities, and so it is convenient to adopt a rate formulation.

Initially, at time $t = 0$, the cavity has a radius (a_0) and an internal pressure (p_0). At time t, later on, the cavity has enlarged and has a current radius (a), while the internal pressure has increased to p. A typical material point of the continuum has now a radial co-ordinate (r), having moved to this position from its original location (r_0). In the absence of body forces, this requirement can be expressed as

$$\frac{\partial \sigma_r}{\partial r} + \frac{\sigma_r - \sigma_\theta}{r} = 0 \tag{3}$$

$$\sigma_r = p \quad \text{at } r = a \tag{4}$$

$$\sigma_r = p_0 \quad \text{at } r = \infty \tag{5}$$

assuming that during cavity expansion, σ_r is the major principal stress, and σ_θ the minor principal stress.

Consider the situation shown schematically in Fig. 4, where the cavity has a radius a, an internal pressure p, and plastic yield is occurring throughout the region $a \le r \le R$. Beyond the elastoplastic interface $r \ge R$, the material remains elastic with Young's modulus E and Poisson's coefficient ν as elasticity parameters.

The cohesive frictional material behavior obeys the Mohr–Coulomb criterion:

$$f = \sigma_r + c \operatorname{cotg} \varphi - N(\sigma_\theta + c \operatorname{cotg} \varphi) = 0 \tag{6}$$

where c is cohesion and

$$N = \frac{1 + \sin \varphi}{1 - \sin \varphi} \tag{7}$$

The constitutive relation in the plastic zone reduces to the single differential equation:

$$\frac{\partial (\mathrm{d}u)}{\partial r} + \frac{1}{M} \frac{\mathrm{d}u}{r} = -2\varepsilon_R \chi \left(\frac{r}{R} \right)^{\beta - 1} \frac{\mathrm{d}R}{R} \tag{8}$$

where

$$\chi = \frac{(1 - \nu) - \nu(M + N) + (1 - \nu)MN}{MN} \tag{9}$$

$$M = \frac{1 + \sin \psi}{1 - \sin \psi} \tag{10}$$

ψ is the dilatancy angle.

Finally, we will find at the elastic–plastic interface ($r = R$):

$$\mathrm{d}u(r = R) = 2\varepsilon_R \, \mathrm{d}R \tag{11}$$

where u is the radial displacement and $\varepsilon_R = (\sigma_R - p_0) \cdot (1 + \nu)/2E$.

Table 2
Necessary model parameters before and after injection.

Depth (m)	E (kPa)	ν (–)	ϕ (°)	k_0 (–)	c (kPa) before injection	c (kPa) after injection
1.5	5000	0.3	30	0.5	70	260
2.5	5000	0.3	30	0.5	160	640
3.5	5000	0.3	30	0.5	40	210
4.0	12000	0.3	30	0.5	350	1100

Then, we obtain:

$$\mathrm{d}u = \left\{ T\left(\frac{R}{r}\right)^{\alpha} - Z\left(\frac{R}{r}\right)^{-\beta} \right\} \varepsilon_R \, \mathrm{d}R \tag{12}$$

where $T = 2(1 + \frac{\chi}{\alpha+\beta})$ and $Z = 2(\frac{\chi}{\alpha+\beta})$.

If the cavity is created in a saturated porous medium, then the total stress should be replaced by the effective stress rate.

4. Model predictions for pressuremeter results

In this section, the proposed solution is applied to predict the pressuremeter results and to interpret the effect of resin injection on the soil behavior.

All the necessary parameters of the model for the soil characteristics before and after injection (Young's modulus E, Poisson's ratio ν, friction angle ϕ, cohesion c, and coefficient of earth pressure at rest k_0) are reported in Table 2.

In order to facilitate the analysis, only the cohesion parameter is modified before and after injection. The fiction angle (ϕ) as well as the elasticity parameters (E, ν) are taken constant, and are independent of the injection process. For the different depths, cohesion after injection is between three and five times more than its initial value.

The initial radius a_0 is taken at 1 cm, and is equal to the radius of the pressuremeter probe. A wet density of 20 kN/m^3 is taken for all the studied soils. The water table is higher than 4 m, and therefore the total stress concept was used in this study.

To obtain the radial stress–expansion curve, it is necessary to calculate the volume change during the pressuremeter test. We propose the following equation for the volume change ΔV:

$$\Delta V = \pi(a_0 + u)^2 h - \pi(a_0)^2 h_0 \tag{13}$$

where u is the predicted model displacement varying with the applied radial stress, a_0 is 1 cm, h_0 and h are the initial and final height of the pressuremeter probe.

We take a coefficient of 8 for the ratio of the height on the radius of probe (h/a). If we rewrite Eq. (24), the volume change can be calculated by:

$$\Delta V = 8\left(\pi(a_0 + u)^3 - \pi(a_0)^3\right) \tag{14}$$

Fig. 5 compares the model prediction with the experimental results. Generally, the results show the good capacity of the analytical solution to reproduce the pressuremeter results before and after injection.

The modeling predictions confirm that the initial elastic part of the curve is not be influenced by the injection process and, therefore, that the same elasticity parameters can be used to describe the elastic behavior of the soil.

5. Model predictions for the cone penetration results

The undrained cohesion value is theoretically given by:

$$C_u = \frac{(\sigma_{r\,\max} - p_0)}{2} \tag{15}$$

where p_0 is the initial mean stress, $\sigma_{r\,\max}$ is the radial stress at the rapture point of the Mohr–Coulomb criterion.

By using Eq. (6), we have:

$$\sigma_{r\,\max} = \left(\frac{1 + \sin\varphi}{1 - \sin\varphi}\right) p_0 + \left(\frac{2\cos\varphi}{1 - \sin\varphi}\right) c \tag{16}$$

And then Eq. (15) becomes:

$$C_u = \left(\frac{\sin\varphi}{1 - \sin\varphi}\right) p_0 + \left(\frac{\cos\varphi}{1 - \sin\varphi}\right) c \tag{17}$$

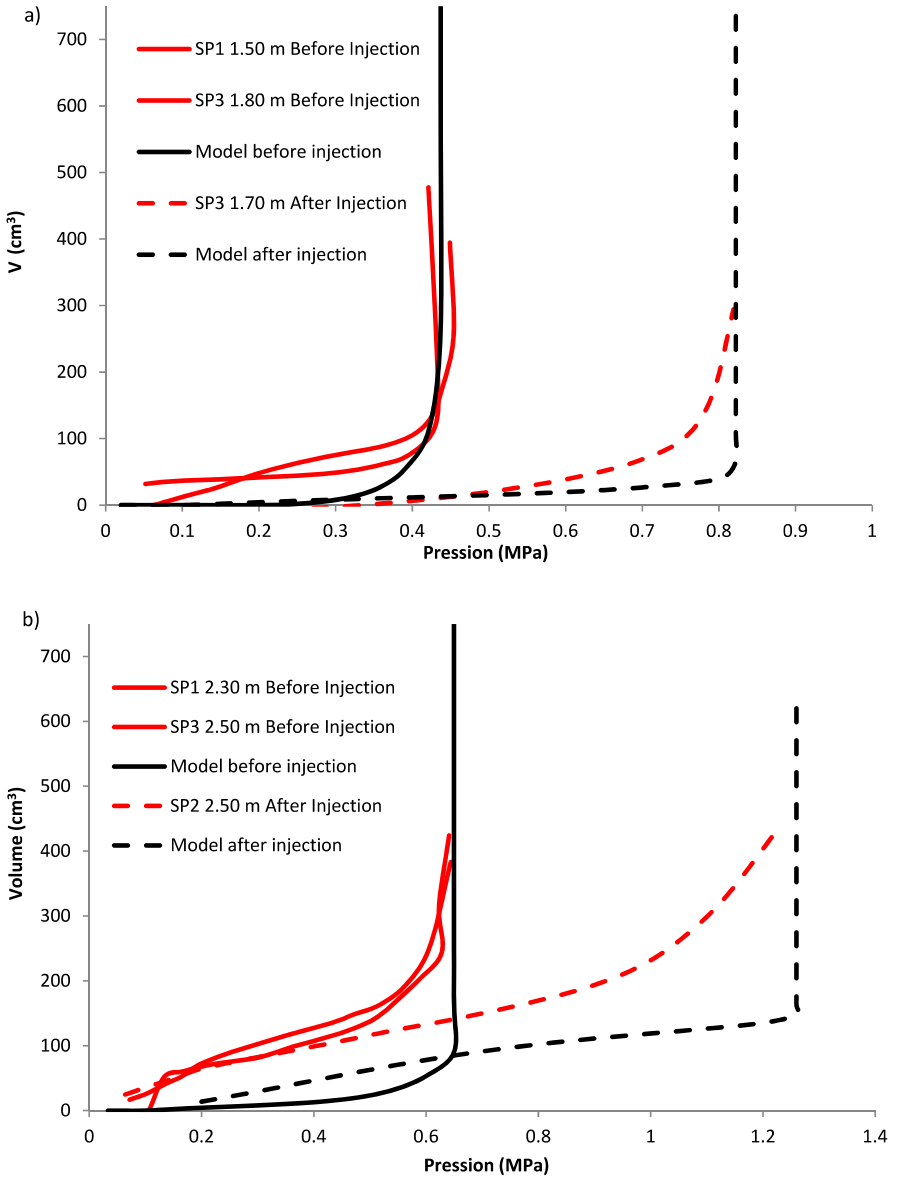

Fig. 5. Model prediction compared with pressuremeter results before and after injection: a) between 1.5 m and 1.8 m, b) between 2.3 m and 2.5 m, c) between 3.1 m and 3.3 m and d) between 4.0 m and 4.2 m.

There are many theoretical solutions for the relation between the soil resistance of the cone penetration test (R_d) with its undrained cohesion such as its bearing capacity theory [27,28], cavity expansion theory [29,30], analytical and numerical approaches [31], or strain path theory [32]. A detailed summary of these methods is given in Lunne et al. [33]. The following simplified relation was used in this study:

$$R_d = 22\, C_u \tag{18}$$

Fig. 6 compares the model estimation for the soil resistance of CP_1 and CP_4 before and after injection compared with the experimental results. It can be observed that the estimated values are globally comparable with the experimental results before injection; however, the experimental values are overestimated for depths less than 3 m and underestimated for depths higher than 3 m. After injection, the model prediction is higher than the experimental values of the CP_4 test (Fig. 6b) because the injected volume of resin for the adjacent points is less than the average values. The model can predict correctly the significant increase in soil resistance for the CP_1 test at a depth of 2 m (Fig. 6a), although the predicted value is still less than the measured value because of the simplified analytical solution assayed in this part. Generally, it can be stated that the model predicts correctly the increase in the undrained cohesion of plastic clays after injection.

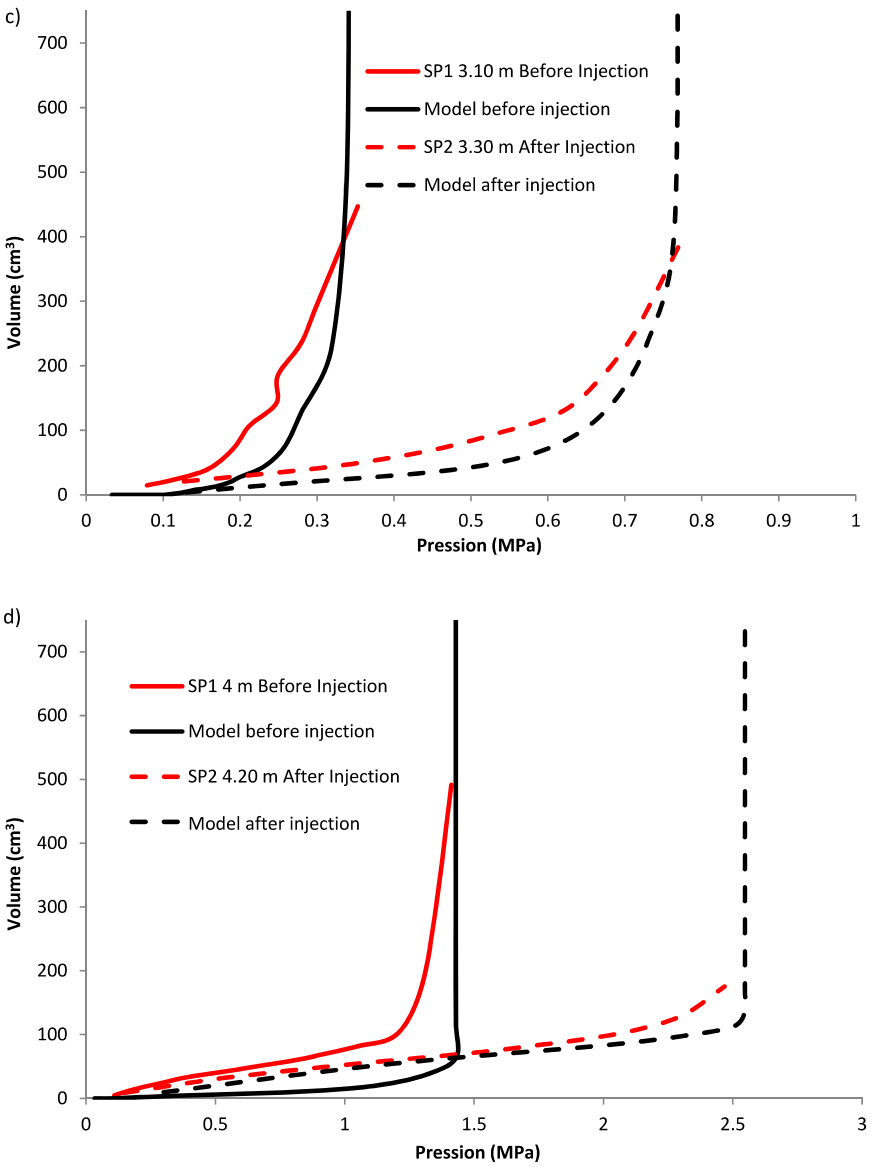

Fig. 5. (*continued*)

Additional experimental tests such as direct shear tests, triaxial test, and oedometer compression tests permit to estimate properly the mechanical characteristics and to improve qualitatively and quantitatively, respectively, the model's predictions.

6. Conclusion

This paper presents the experimental results for pressuremeter and cone penetration tests before and after resin injection in clays with high plasticity. It can be globally observed a very important increase in the pressure limit or in the soil resistance for all the depths studied close to the injection points.

To interpret the experimental results, an analytical analysis for cylindrical pore cavity expansion in cohesive frictional soils with the Mohr–Coulomb criterion was then used. The model parameters were calibrated where the cohesion values before and after injection were modified and the elasticity parameters as well as the friction angle were taken constant. The calibrated parameters reproduce well the pressuremeter results before and after injection at the different depths. A significant increase in cohesion was observed because of soil densification after resin expansion for all the studied depths. A factor between 4 and 5 can be proposed for the cohesion increase after injection.

The estimated undrained cohesions of the model were also used to estimate the cone penetration tests before and after injection. Globally, the model predictions show the efficiency of resin injection in clay soils. However, a better analytical solution as well as additional laboratory tests may improve the quality of the predicted results.

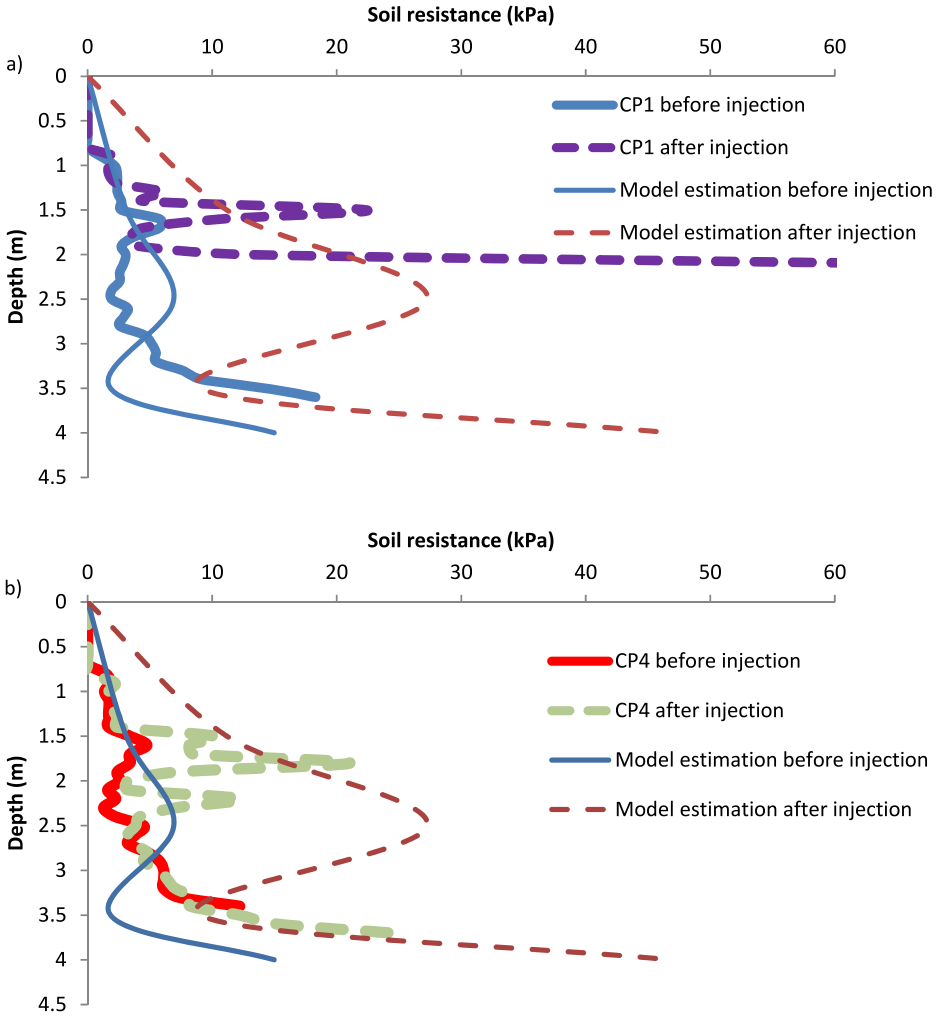

Fig. 6. Model estimation compared with cone penetration results before and after injection a) for the CP1 test and b) for the CP4 test.

This work is a preliminary attempt at studying the field effect of resin injection on the behavior of clay soils. Further points such as the optimum injection volume and its propagation in clays, the unsaturated state of clay soils before injection or the modification in the structure of the clay after injection are still necessary to be considered to complete this study.

Acknowledgements

This work was funded by the Solinjection Company (Special thanks to M. Tabatabaei) and the experimental tests were performed by GeoEST (special thanks are due to M. Hosseini).

References

[1] O. Buzzi, S. Fityus, Y. Sasaki, S. Sloan, Structure and properties of expanding polyurethane foam in the context of foundation remediation in expansive soil, Mech. Mater. 40 (2008) 1012–1021.
[2] O. Buzzi, S. Fityus, S. Sloan, Use of expanding polyurethane resin to remediate expansive soil foundations, Can. Geotech. J. 47 (6) (2010) 623–634.
[3] R. Valentino, E. Romeo, A. Misra, Mechanical aspects of micropiles made of reinforced polyurethane resins, Geotech. Geolog. Eng. 31 (2013) 463–478.
[4] R. Valentino, E. Romeo, D. Stevanoni, An experimental study on the mechanical behaviour of two polyurethane resins used for geotechnical applications, Mech. Mater. 71 (2014) 101–113.
[5] Z.H. Tu, V.P.W. Shim, C.T. Lim, Plastic deformation modes in rigid polyurethane foam under static loading, Int. J. Solids Struct. 38 (2001) 9267–9279.
[6] N.C. Hilyard, A. Cunningham, Low Density Cellular Plastics, Chapman & Hall, London, 1994.
[7] L.J. Gibson, M.F. Ashby, Cellular Solids, Cambridge University Press, Cambridge, UK, 1997.
[8] C.M. Ford, L.J. Gibson, Uniaxial strength asymmetry in cellular materials: an analytical model, Int. J. Mech. Sci. 40 (6) (1998) 521–531.
[9] ASTM D4719-07, Standard Test Methods for Prebored Pressuremeter Testing in Soils, ASTM International, West Conshohocken, PA, USA, 2007.
[10] ASTM D3441-05, Standard Test Method for Mechanical Cone Penetration Tests of Soil, ASTM International, West Conshohocken, PA, USA, 2005.
[11] G.S. Hollabaugh, J.M. Dees, Propellant Gas Fracture Stimulation of a Horizontal Austin Chalk Wellbore. Presented at the SPE Annual Technical Conference and Exhibition, Houston, Texas, 3–6 October 1993, SPE-26584-MS, http://dx.doi.org/10.2118/26584-MS.

[12] J.M. Dees, P.J. Handren, A new method of overbalanced perforating and surging of resin for sand control, J. Pet. Technol. 46 (5) (1994) 431–435, http://dx.doi.org/10.2118/26545-PA, SPE-26545-PA.
[13] R.E. Gibson, W.F. Anderson, In situ measurement of soil properties with the pressuremeter, Civil Eng. Public Works Rev. 56 (1961) 615–618.
[14] P. Chadwick, The quasi-static expansion of a spherical cavity in metals and ideal soils, Q. J. Mech. Appl. Math. (1) XII (1959) 52–71.
[15] A.C. Palmer, Undrained plane–strain expansion of a cylindrical cavity in clay: a simple interpretation of the pressuremeter test, Géotechnique 22 (3) (1972) 451–457.
[16] A.S. Vesic, Expansion of cavities in infinite soil mass, J. Soil Mech. Found. Div. 98 (3) (1972) 265–290.
[17] J.M.O. Hughes, C.P. Wrath, D. Windle, Pressuremeter tests in sands, Géotechnique 27 (4) (1977) 455–477.
[18] M.F. Randolph, J.P. Carter, C.P. Wrath, Driven piles in clay – the effects of installation and subsequent consolidation, Géotechnique 29 (4) (1979) 361–393.
[19] J.P. Carter, S.K. Yeung, Analysis of cylindrical cavity expansion in a strain weakening material, Comput. Geotech. 1 (1985) 161–180.
[20] I.P. Carter, J.R. Booker, S.K. Yeung, Cavity expansion in cohesive frictional soils, Géotechnique 36 (3) (1986) 349–358.
[21] H.S. Yu, G.T. Houlsby, Finite cavity expansion in dilatant soils: loading analysis, Géotechnique 41 (2) (1991) 173–183.
[22] J.-F. Zou, H. Luo, L. Li, Mechanism analysis of fracture grouting in soil with large strain considering intermediate principal stress, J. Rock Soil Mech. 29 (9) (2008) 2515–2520.
[23] I.F. Collins, J.R. Stimpson, Similarity solutions for drained and undrained cavity expansions in soils, Géotechnique 44 (1) (1994) 21–34.
[24] L.F. Cao, C.I. Teh, M.F. Chang, Undrained cavity expansion in modified Cam clay I: theoretical analysis, Géotechnique 51 (4) (2001) 323–334.
[25] A. Dei Svaldi, M. Favaretti, A. Pasquetto, G. Vinco, Analytical modelling of the soil improvement by injections of high expansion pressure resin, Bull. Angew. Geol. 10 (2) (2005) 71–81.
[26] S.L. Chen, N.Y. Abousleiman, Exact undrained elasto-plastic solution for cylindrical cavity expansion in modified Cam Clay soil, Géotechnique 62 (5) (2012) 447–456.
[27] K. Terzaghi, Theoretical Soil Mechanics, John Wiley and Sons, 1943.
[28] E. De Beer, Static cone penetration testing in clay and loam, in: Proceedings of Sonder Symposium, Fugro, Sonder Symposium, 1977, pp. 15–23.
[29] A. Skempton, The bearing capacity of clays, in: Proceedings of the Building Research Congress, Building Research Congress, National Research Council, 1951, pp. 180–189.
[30] A. Vesic, Principles of Pile Foundation Design, Duke University, Durham, NC, USA, 1975.
[31] B. Ladanyi, Deep punching of sensitive clays, in: Proceedings of the 3rd Pan American Conference on Soil Mechanics and Foundation Engineering, 3rd Pan American Conference on Soil Mechanics and Foundation Engineering, Sociedad Venezolana de Mecánica del Suelo e Ingeniería de Fundaciones, 1967, pp. 533–546.
[32] C. Teh, An analytical study of the cone penetration test, PhD thesis, Oxford University, Oxford, UK, 1987.
[33] T. Lunne, P.K. Robertson, J.J.M. Powell, Cone Penetration Testing in Geotechnical Practice, Blackie Academic/Routledge Publishing, New York, 1997.